International Journal of Automotive Technology, Vol. 5, No. 2, pp. 109–114 (2004)

1229–9138/2004/016–05

HUMAN-IN-THE-LOOP EVALUATION OF A VEHICLE STABILITY CONTROLLER USING A VEHICLE SIMULATOR

T. CHUNG[1], J. KIM[2] and K. YI[3]*

[1]Department of Automotive Engineering, Hanyang University, Seoul 133-791, Korea
[2]Brake R&D Department, Hyundai Mobis, 80-10 Mabuk-ri, Guseong-eup, Yongin-si, Gyeonggi-do 449-912, Korea
[3]School of Mechanical Engineering, Hanyang University, Seoul 133-791, Korea

(Received 15 September 2003; Revised 25 January 2004)

ABSTRACT–This paper presents a closed-loop evaluation of the Vehicle Stability Control (VSC) system using a vehicle simulator. Human driver-VSC interactions have been investigated under realistic operating conditions in the laboratory. Braking control inputs for vehicle stability enhancement have been directly derived from the sliding control law based on vehicle planar motion equations with differential braking. A driving simulator has been validated using actual vehicle driving test data. Real-time human-in-the loop simulation results in realistic driving situations have shown that the proposed controller reduces driving effort and enhances vehicle stability.

KEY WORDS : Human-in-the-loop evaluation, Driving simulator, Real-time simulation, Vehicle stability control (VSC) systems, Sliding mode control

1. INTRODUCTION

The Vehicle Stability Control (VSC) system is an active safety system for road vehicles which stabilizes the vehicle dynamic behavior in emergency situations such as spinning, drift out and roll over (Van Zanten, 1996). In this study, we have examined VSC systems from two points of view: an evaluation method of the VSC system and the design of a 3-D vehicle model based sliding controller.

VSC systems connect the human driver, controller and vehicle behavior (Chen and Peng, 2001). Since VSC always works with the driver, the overall vehicle performance will depend on not how well the VSC works, but rather its interaction with the human driver. It is hard to predict driver input with a mathematical driver model. It is also difficult to test an actual vehicle due to time and costs. Therefore, we applied a driving simulator to evaluate the system. If the driving simulator can simulate the actual driving situations well, the human-in-the-loop evaluation makes sense. The driving simulator consists of a three dimensional vehicle dynamic model, driver interface and a visual display (Lee *et al.*, 2003). It was validated by the drivers input data of actual vehicle test data.

Secondary, we introduce a 3-DOF vehicle model based sliding controller. Most of Direct Yaw Moment controllers are based on a 2-DOF model which is derived from the assumption that longitudinal vehicle velocity is constant (Tseng *et al.*, 1999). Since lateral and longitudinal motions of a vehicle are governed by longitudinal and lateral tire forces, VSC systems need to be designed using a 3-DOF vehicle yaw plane model including vehicle longitudinal motion with inputs of brake forces of each wheel. Sliding surface is defined as yaw rate error and vehicle side slip angle, and brake input is directly derived from the sliding control law based on vehicle planar model with differential braking.

We apply the 3-DOF model based sliding controller to the driving simulator, and test under some critical driving situations. The controller is tested under circular track driving, slalom and emergency lane changing situations to examine how the VSC system affects to reactions of the driver.

2. VALIDATION OF HUMAN-IN-THE-LOOP SYSTEM

This section describes the configurations of a human-in-the-loop evaluation system and its validation. Although this method does not exactly predict the response of the physical and mental systems of the human driver, the model does correlate well with trends observed from vehicle test results of driver's responses under certain

*Corresponding author. e-mail: Kyongsu@hanyang.ac.kr

driving conditions.

2.1. Configurations of Driving Simulator

Figure 1 shows the schematic diagram and vehicle-driver interface of the driving simulator. Real-time simulation environment of the driving simulator is implemented by using Matlab xPC target that provides real-time kernel on the real-time simulation PC (Uematsu and Gerdes, 2002). During real-time simulations, real-time simulation PC calculates the variables of vehicle model controlled by VSC algorithm with sensed driver's reactions. Then, it provides vehicle motions such as position, yaw, roll and pitch angle to a 3-D Animation PC, which displays visual information of a driving situation. Driver's responses are acquired through brake pressure sensor, steering wheel angle sensor and throttle angle sensor. The wide-view monitor shows the 3D animation of a driving situation. Actual vehicle parts such as dashboard, steering wheel, brake pedal, accelerator pedal and driver's seat are equipped.

The full vehicle dynamic model performs real-time simulations in the driving simulator. The proposed vehicle model consists of a vehicle body, suspension, nonlinear tire model and powertrain models as shown in Figure 2. The vehicle body with 6-DOF is connected to 4-quarter car suspensions with roll bar. The powertrain model includes static engine and torque converter models, an automatic transmission with gearshift map and driving shafts. Pacejka's tire model has been used to compute the

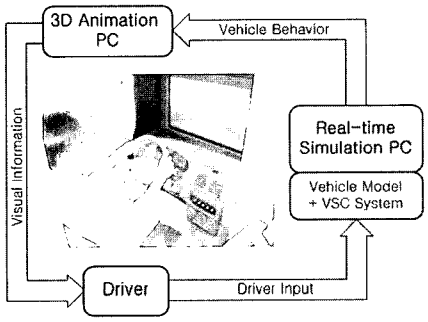

Figure 1. Schematics of human-in-the-loop system.

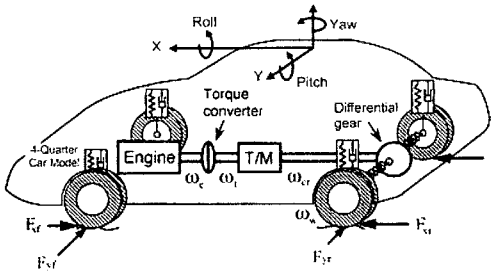

Figure 2. Full vehicle dynamic model.

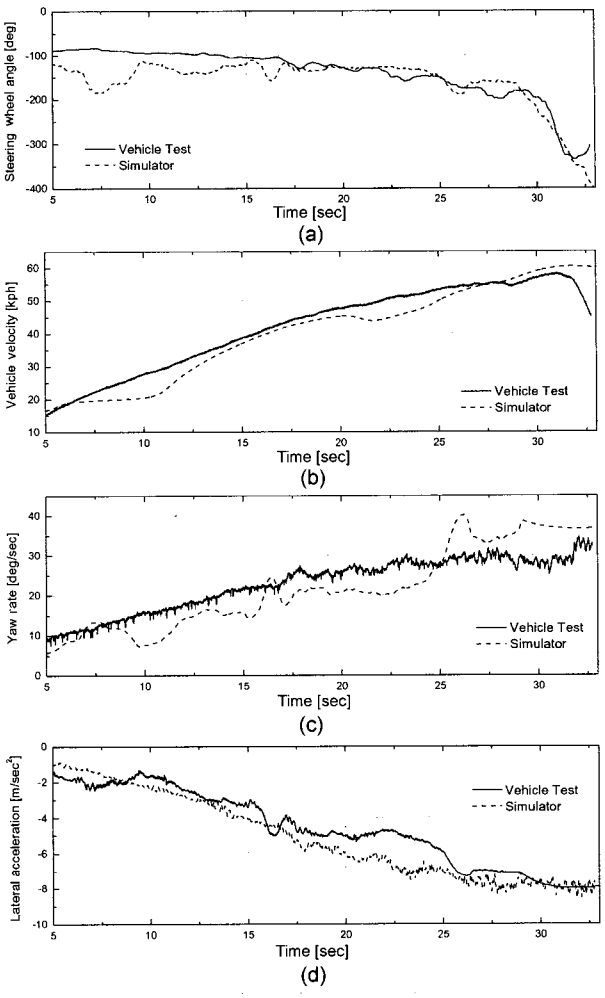

Figure 3. Comparison between simulator and test data (circular track driving).

tire forces of each wheel (Ha *et al.*, 2003).

2.2. Results of Driver Responses

This section describes the driver's response in the driving simulator and actual vehicle test for circular track driving and a slalom test on normal road conditions.

2.2.1. Increasing speed on a circular track

Vehicle test data on a 30m-radius circular road have been used to validate the driving simulator. Figure 3 shows a comparison between vehicle test data and simulator driving data.

The vehicle speed has been increased until the vehicle's drifting out from the circular road as shown in Figure 4(B). Figure 4(A) and 4(B) show that the driver steers abruptly at a vehicle speed of 55 kph in order to follow the track. Comparisons of lateral accelerations and yaw rates of the vehicle are shown in Figures 4(C) and

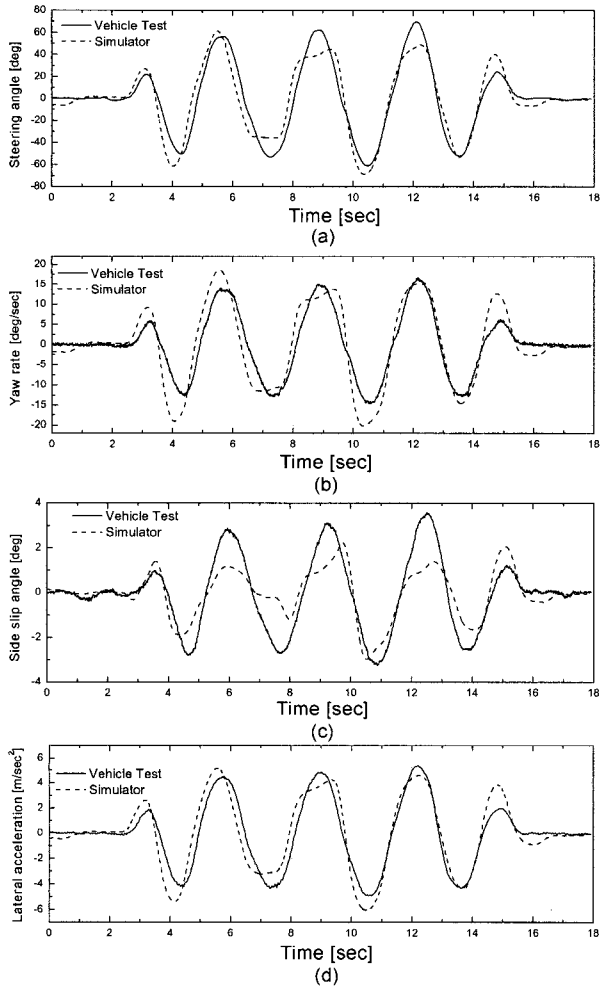

Figure 4. Comparison between simulator and actual vehicle test data (slalom I).

4(d). When vehicle speed is increased similar to the actual vehicle test results, driver steering response of driving simulator is quite similar with vehicle test results.

2.2.2. Slalom maneuver

The slalom test is conducted to examine vehicle cornering properties. The driver keeps an approximately constant vehicle speed about 60 kph. The cone width is 30m. Figures 4 and 5 show that the results of slalom test as time histories.

The magnitude and frequency of the driver steering input are almost identical in both the vehicle test results and driving simulator (Figure 4(a)). The vehicle responses, yaw rate, side slip angle and lateral acceleration are also quite similar to the actual test results as shown in Figures 4(b), (c), (d). Figure 5 shows that the results as phase plot in dependence of the lateral acceleration of the vehicle. The maximum value of lateral acceleration and steering

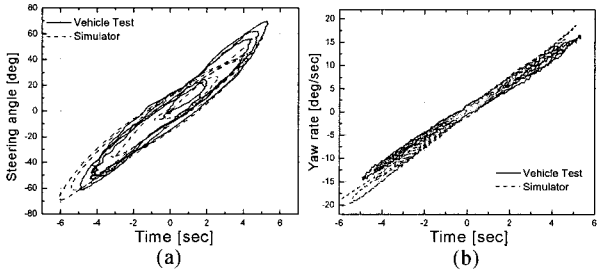

Figure 5. Comparison between simulator and actual vehicle test data (slalom II).

wheel angle (Figure 5(a)), and the slope between yawrate and lateral acceleration are almost the same (Figure 5(b)).

The comparison between the driving simulator and vehicle test results shows that the proposed driving simulator is very feasible for describing actual vehicle dynamic behaviors. It means that the driving simulator accurately reproduces actual driving conditions.

3. DESIGN OF 3-DOF VEHICLE MODEL BASED SLIDING CONTROLLER

A differential braking control law for the VSC based on three-degree of freedom vehicle planar motions has been evaluated in this study.

3.1. Vehicle Planar Motion Model

The vehicle model used in this study is a 3-DOF vehicle yaw plane representation with differential braking and equations of motions describing vehicle yaw plane model are as follows:

$$m\dot{u}=F_{xr}+F_{xf}\cos\delta-F_{yf}\sin\delta+mrv$$

$$m\dot{v}=F_{yr}+F_{xf}\sin\delta-F_{yf}\cos\delta-mru$$

$$I_z\dot{r}=aF_{xf}\sin\delta+aF_{yf}\cos\delta-bF_{yr}$$
$$+d/2\cdot(F_{xfr}-F_{xfl})\cos\delta+d/2\cdot(F_{xrr}-F_{xrl}) \quad (1)$$

where u is longitudinal vehicle velocity, v is lateral vehicle velocity and γ is yaw rate. F_x and F_y are longitudinal and lateral tire forces. The suffix *fr*, *fl* is front right, front left and *rr*, *rl* is rear right, rear left. The front and rear tire slip angles, α_f and α_r are average slip angles of the left and right wheels. δ is steering angle input. a and b are distances from the center of gravity to front and real axle, d is track width. m represents vehicle mass, and I_z is moment of inertia about yaw axis.

3.2. Sliding Control Law

The desired value of the yaw rate (γ_{des}) is computed based on the driver's steering input and vehicle longitudinal speed using a linear tire model (Chen and Peng,

2001). Since the lateral acceleration is limited by the friction coefficient between the tires and the road, the desired yaw rate is also limited under the value of $\mu g/u$. μ represents the friction coefficient between the road and tire. The sliding surface is defined as a weighted combination of the side slip angle and the difference between the yawrate and desired yawrate such that

$$s=r_{des}-r+\rho-\beta \tag{2}$$

Where, ρ is a positive constant (Uematsu and Gerdes, 2002). The control objective is to keep the scalar, S, at zero and this can be achieved by choosing the control law such that

$$\dot{s}=-K\cdot s \tag{3}$$

Where, K is a positive constant. Equation (3) is easily obtained by substitutions of equations (1) and (2). The tire longitudinal forces can be controlled by wheel braking control. Since the wheel dynamics are faster than vehicle body dynamics, assuming front driving, the tire longitudinal forces can be approximated as

$$F_{xf}=F_{xfl}+F_{xfr}\cong\frac{T_s}{r_{wf}}-(F_{Bfl}+F_{Bfr})$$
$$F_{xr}=-(F_{Brl}+F_{Brr}) \tag{4}$$

Where T_s represents driving shaft torque and F_B is the braking forces of each wheel. Rear brake forces are calculated by proportioning of the front brake force with respect to longitudinal acceleration. Then equation (3) is represented by the F_B, and we can directly derive the equation for brake input. Left and right brake inputs have to be calculated respectively, and the positive value of the input is applied to the wheel (Yi *et al.*, 2003).

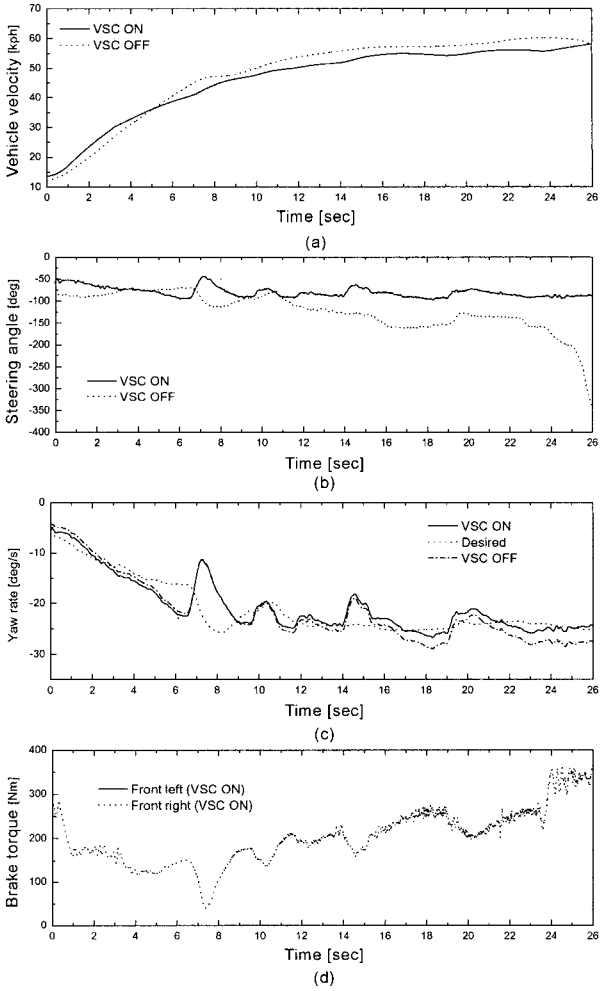

Figure 6. Vehicle responses (circular track).

4. CLOSED-LOOP EVALUATIONS OF VSC SYSTEMS

The proposed vehicle stability controller has been evaluated via closed-loop method using the driving simulator. The driver conducted circular track driving and emergency lane change cases with or without the proposed VSC system.

4.1. Circular Track Driving

Figure 6 shows the test results using the driving simulator. The driver increases vehicle speed and corrects the steering wheel angle to make the vehicle follow the track with a 30 radius of curvature in a clockwise direction. Figure 6(a) shows the vehicle velocity. Without VSC, the driver's steering wheel angle is diverged at 60 kph as shown in Figure 6(b). With VSC, the longitudinal velocity is limited by the brake input and the yaw rate follows the desired value. Figure 6(d) shows brake torque applied to the front wheels. The brake torques of the right wheels has been controlled in order to stabilize the vehicle.

4.2. Emergency Lane Change Maneuvers

A single lane change test has been conducted on normal road and low-μ road at 120 kph. Under an assumption of sudden cut-in situation of a previous vehicle or other obstacles, the driver performs the single lane change maneuver within 2 seconds.

4.2.1. Lane change on normal road

The driver changes a lane promptly when the vehicle speeds are about 120 kph. Without VSC, a driver steers more to change the lane, and has difficulty stabilizing after the lane change (Figure 7(a)). With VSC, the brake inputs are generated on both wheels in turns through the lane change maneuver as shown in Figure 7(b). To prevent wheel locking, front brake torques are limited about 110, based on the friction coefficient of the road.

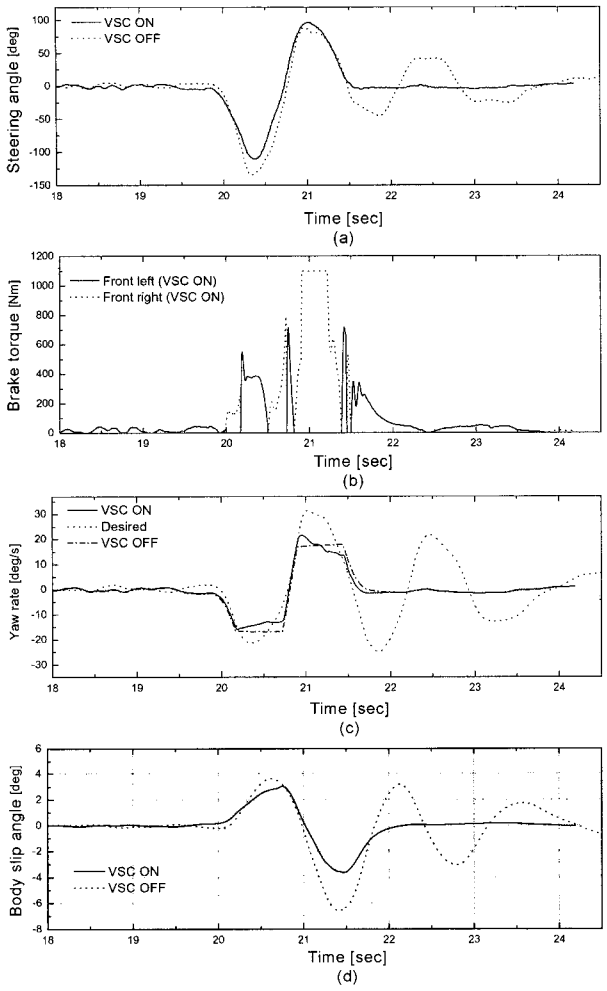

Figure 7. Vehicle responses (lane change, high-μ).

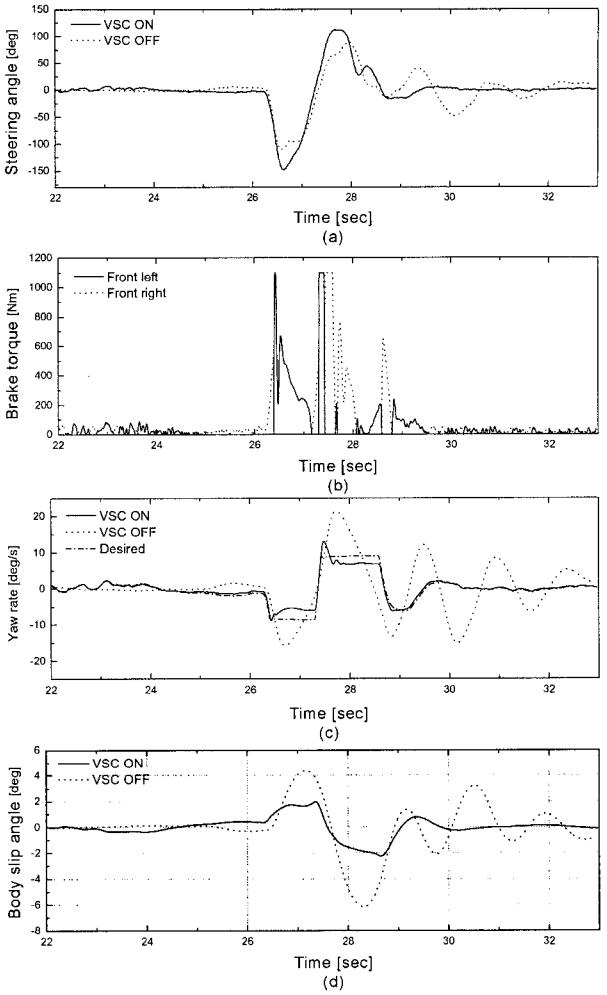

Figure 8. Vehicle responses (lane change, low-μ).

The desired yaw rate is limited to about the peak steering wheel angle, but the yaw rate follows the desired value with VSC. The behavior of the controlled vehicle is more stable with respect to yaw rate and body slip angle as shown in Figure 7(c) and (d). It can be seen that the controller exhibits superior handling performance. The driver feels better as his steering effort is reduced to stabilize the vehicle with the VSC.

4.2.2. Lane change on low friction road

In this case, the driver changes a lane at 120 kph on a low-μ road. Less lateral tire force is generated for this road condition, and more steering wheel angle is needed in this case. The driver perfoms more steering with a VSC controller, but less effort in stabilizing after the lane change like the previous result as shown in Figure 8(a). In case of the VSC ON, brake inputs have been applied with higher frequency to reduce side slip angle (Figure 8 (b)). The yaw rate of the vehicle shows more overshoot with respect to the limited desired value than in the high-μ case, but it follows desired value well as shown in Figure 8(c). In the case of VSC ON, body slip angle is regulated within 2 degrees (Figure 8(d)). The controlled vehicle shows transient response, but it does not lose controllability.

4.3. Slalom Maneuver

To examine cornering characteristics, slalom tests with and without VSC are presented. Both actual vehicle test and driving simulator results are performed at 60 kph on a normal road. The steering wheel angle is limited within 150 degrees with VSC as shown in Figure 9(a). Without VSC, the driver steers more than 300 degrees. It represents that about 75 kph is velocity limit of 30 m-cone-width slalom test with a conventional vehicle. With VSC case, the vehicle speed regulated by the VSC around 75 kph without driver's braking. The control input is presented in Figure 9(b). Without VSC, driver reduces vehicle speed immediately at 25 sec to maintain the

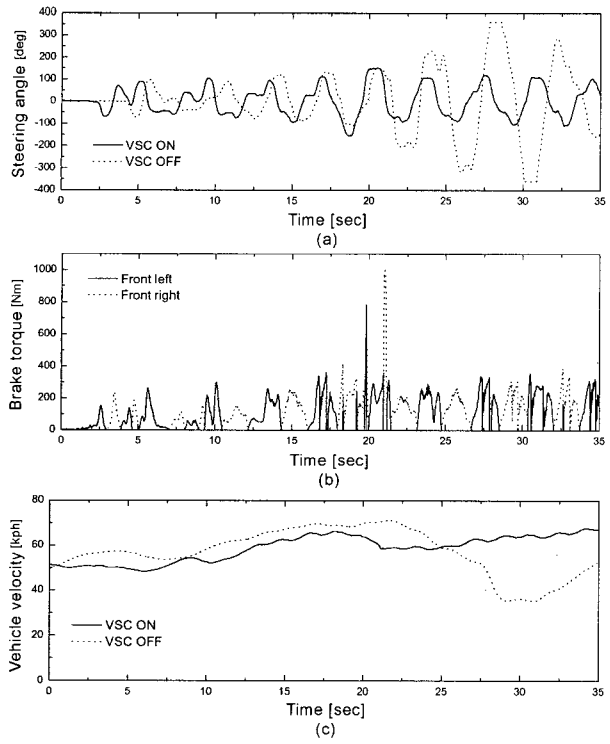

Figure 9. Vehicle responses (slalom I).

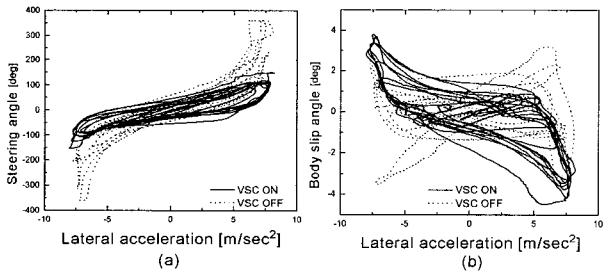

Figure 10. Vehicle responses (slalom II).

slalom path (Figure 9(c)).

Figure 10 shows the results based on the lateral acceleration of the vehicle. As shown in Figure 10(a), less steering wheel angle is needed to generate the same level of lateral tire forces in the VSC ON case. When the vehicle possesses a positive lateral acceleration, the body slip angle tends to be negative. As shown in Figure 10(b), the result does not agree with this tendency in the VSC OFF case.

5. CONCLUSION

The Human-in-the-loop method has been used to evaluate the 3-DOF model based VSC system. Human driver-VSC interactions have been investigated under realistic operating conditions in the laboratory. The driver's responses in nearly same driving conditions are almost idendical between the driving simulator and actual vehicle test. It shows that the driving simulator and its vehicle dynamic model acculately predict the response of a driver. Real-time human-in-the-loop simulation results for critical driving situations have shown that the proposed controller reduces driving effort and enhances stability of the vehicle. Since the human driver-vehicle-VSC interactions can be evaluated by the driving simulator, the closed-loop evaluation method proposed in this paper can be a powerful tool for the development of the VSC systems.

ACKNOWLEDGMENTS–This research has been supported by the Ministry of Science and Technology of Korea in the form of NRL Project. The authors would like to acknowledge the cooperation of the Hyundai Mobis.

REFERENCES

Chen, B. and Peng, H. (2001). Differential-braking-based rollover prevention for sport utility vehicles with human-in-the-loop evaluations. *Vehicle System Dynamics* **36, 4/5,** 359–389.

Ha, J. S., Chung, T. Y., Kim, J. T., Yi, K. S. and Lee, J. M. (2003). Validation of 3D vehicle model and driver steering model with vehicle test. *Spring Conference Proceeding of KSAE* **2,** 676–681.

Lee, S. J., Kim, Y. J., Park, K. H. and Kim, D. G. (2003). Development of hardware-in-the-loop simulator and vehicle dynamic model for testing ABS. *SAE Paper No.* 2003-01-0858, 63–68.

Tseng, H. E., Ashrafi, B., Madau, D., Brown, T. A. and Recker, D. (1999). The development of vehicle stability control at ford. *IEEE/ASME Transactions of Mechatronics* **4, 3,** 223–234.

Uematsu, K. and Gerdes, J. C. (2002). A comparison of several sliding surfaces for stability control. *AVEC'02* 20024578.

Van Zanten, A. T., Erhardt, R., Pfaff, G., Kost, F., Hartmann, U. and Ehret, T. (1996). Control aspects of the Bosch-VDC, *AVEC96*, 573–607.

Yi, K. S., Chung, T. Y., Kim, J. T. and Yi, S. J. (2003). An Investigation into differential braking strategies for vehicle stability control. *Proc. of the Institution of Mechanical Engineers Pard D: Journal of Automobile Engineering* **217,** 1071–1093.